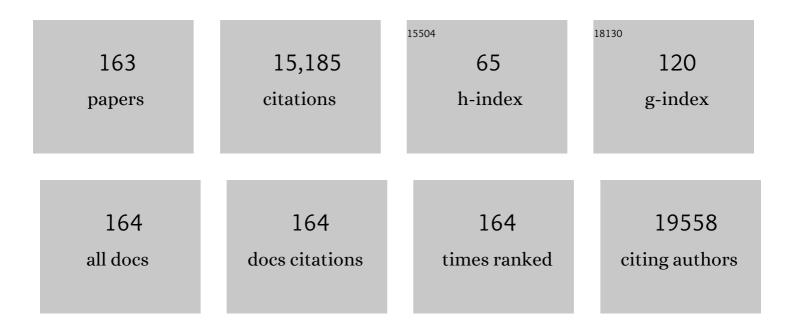


List of Publications by Year in descending order

Source: https://exaly.com/author-pdf/3131305/publications.pdf Version: 2024-02-01



#	Article	IF	CITATIONS
1	Toward New Forms of Particle Sensing and Manipulation and 3D Imaging on a Smartphone for Healthcare Applications. Advanced Photonics Research, 2022, 3, 2100106.	3.6	Ο
2	Ultrafastâ€Response/Recovery Flexible Piezoresistive Sensors with DNA‣ike Double Helix Yarns for Epidermal Pulse Monitoring. Advanced Materials, 2022, 34, e2104313.	21.0	63
3	Ion Migration in Perovskite Lightâ€Emitting Diodes: Mechanism, Characterizations, and Material and Device Engineering. Advanced Materials, 2022, 34, e2108102.	21.0	85
4	Crosstalkâ€Free, Highâ€Resolution Pressure Sensor Arrays Enabled by Highâ€Throughput Laser Manufacturing. Advanced Materials, 2022, 34, e2200517.	21.0	27
5	Anisotropic Charge Transport Enabling Highâ€īhroughput and Highâ€Aspectâ€Ratio Wet Etching of Silicon Carbide. Small Methods, 2022, 6, .	8.6	27
6	Diammoniumâ€Mediated Perovskite Film Formation for High‣uminescence Red Perovskite Lightâ€Emitting Diodes. Advanced Materials, 2022, 34, .	21.0	23
7	PCA-Based Multi-Wavelength Photoplethysmography Algorithm for Cuffless Blood Pressure Measurement on Elderly Subjects. IEEE Journal of Biomedical and Health Informatics, 2021, 25, 663-673.	6.3	27
8	How Far Are We from Achieving Selfâ€Powered Flexible Health Monitoring Systems: An Energy Perspective. Advanced Energy Materials, 2021, 11, 2002646.	19.5	70
9	Unveiling the crystalline packing of Y6 in thin films by thermally induced "backbone-on―orientation. Journal of Materials Chemistry A, 2021, 9, 17030-17038.	10.3	22
10	Phenylalkylammonium passivation enables perovskite light emitting diodes with record high-radiance operational lifetime: the chain length matters. Nature Communications, 2021, 12, 644.	12.8	109
11	Achieving a sub-10 nm nanopore array in silicon by metal-assisted chemical etching and machine learning. International Journal of Extreme Manufacturing, 2021, 3, 035104.	12.7	27
12	Excess Ion-Induced Efficiency Roll-Off in High-Efficiency Perovskite Light-Emitting Diodes. ACS Applied Materials & Interfaces, 2021, 13, 28546-28554.	8.0	27
13	Ultraâ€Narrowband Photodetector with High Responsivity Enabled by Integrating Monolayer Jâ€Aggregate Organic Crystal with Graphene. Advanced Optical Materials, 2021, 9, 2100158.	7.3	15
14	Integration of Colloidal Quantum Dots with Photonic Structures for Optoelectronic and Optical Devices. Advanced Science, 2021, 8, e2101560.	11.2	35
15	Antidepressant Monotherapy and Combination Therapy with Acupuncture in Depressed Patients: A Resting-State Functional Near-Infrared Spectroscopy (fNIRS) Study. Neurotherapeutics, 2021, 18, 2651-2663.	4.4	19
16	Non-Invasive Capillary Blood Pressure Measurement Enabling Early Detection and Classification of Venous Congestion. IEEE Journal of Biomedical and Health Informatics, 2021, 25, 2877-2886.	6.3	7
17	Interfacial Laserâ€Induced Graphene Enabling Highâ€Performance Liquidâ~'Solid Triboelectric Nanogenerator. Advanced Materials, 2021, 33, e2104290.	21.0	120
18	Sensitive, High‧peed, and Broadband Perovskite Photodetectors with Builtâ€In TiO ₂ Metalenses. Small, 2021, 17, e2102694.	10.0	4

#	Article	IF	CITATIONS
19	Interface Engineering of Flexible Piezoresistive Sensors via Nearâ€Field Electrospinning Processed Spacer Layers. Small Methods, 2021, 5, e2000842.	8.6	29
20	Feasibility of Fingertip Oscillometric Blood Pressure Measurement: Model-Based Analysis and Experimental Validation. IEEE Journal of Biomedical and Health Informatics, 2020, 24, 533-542.	6.3	9
21	A highly stretchable and conductive composite based on an emulsion-templated silver nanowire aerogel. Journal of Materials Chemistry A, 2020, 8, 1724-1730.	10.3	32
22	Role of Excess FAI in Formation of Highâ€Efficiency FAPbI ₃ â€Based Lightâ€Emitting Diodes. Advanced Functional Materials, 2020, 30, 1906875.	14.9	44
23	Understanding Charge Transport in All-Inorganic Halide Perovskite Nanocrystal Thin-Film Field Effect Transistors. ACS Energy Letters, 2020, 5, 2614-2623.	17.4	39
24	Alkali-cation-enhanced benzylammonium passivation for efficient and stable perovskite solar cells fabricated through sequential deposition. Journal of Materials Chemistry A, 2020, 8, 19357-19366.	10.3	13
25	Broad-Band Photodetectors Based on Copper Indium Diselenide Quantum Dots in a Methylammonium Lead Iodide Perovskite Matrix. ACS Applied Materials & Interfaces, 2020, 12, 35201-35210.	8.0	21
26	Ternary Blending Driven Molecular Reorientation of Non-Fullerene Acceptor IDIC with Backbone Order. ACS Applied Energy Materials, 2020, 3, 10814-10822.	5.1	15
27	Nearâ€Field Electrospinning Enabled Highly Sensitive and Anisotropic Strain Sensors. Advanced Materials Technologies, 2020, 5, 2000550.	5.8	18
28	Solution Processed Hybrid Polymer: HgTe Quantum Dot Phototransistor with High Sensitivity and Fast Infrared Response up to 2400Ânm at Room Temperature. Advanced Science, 2020, 7, 2000068.	11.2	52
29	Stabilizing Perovskite Lightâ€Emitting Diodes by Incorporation of Binary Alkali Cations. Advanced Materials, 2020, 32, e1907786.	21.0	64
30	Bidirectional optical signal transmission between two identical devices using perovskite diodes. Nature Electronics, 2020, 3, 156-164.	26.0	126
31	Degradation Mechanism of Perovskite Lightâ€Emitting Diodes: An In Situ Investigation via Electroabsorption Spectroscopy and Device Modelling. Advanced Functional Materials, 2020, 30, 1910464.	14.9	41
32	High Performance Flexible Transparent Electrode via Oneâ€Step Multifunctional Treatment for Ag Nanonetwork Composites Semiâ€Embedded in Lowâ€Temperatureâ€Processed Substrate for Highly Performed Organic Photovoltaics. Advanced Energy Materials, 2020, 10, 1903919.	19.5	58
33	Organic Photovoltaics: High Performance Flexible Transparent Electrode via Oneâ€Step Multifunctional Treatment for Ag Nanonetwork Composites Semiâ€Embedded in Lowâ€Temperatureâ€Processed Substrate for Highly Performed Organic Photovoltaics (Adv. Energy) Tj ETQq1 1 (0. 7 845314	rgBT /Overlo
34	Upconversion nanoparticles extending the spectral sensitivity of silicon photodetectors to λ = 1.5 μm. Nanotechnology, 2020, 31, 495201.	2.6	4
35	Enhanced Incorporation of Guanidinium in Formamidiniumâ€Based Perovskites for Efficient and Stable Photovoltaics: The Role of Cs and Br. Advanced Functional Materials, 2019, 29, 1905739.	14.9	41
36	Integrated Plasmonic Infrared Photodetector Based on Colloidal HgTe Quantum Dots. Advanced Materials Technologies, 2019, 4, 1900354.	5.8	36

#	Article	lF	CITATIONS
37	Core-dependent properties of copper nanoclusters: valence-pure nanoclusters as NIR TADF emitters and mixed-valence ones as semiconductors. Chemical Science, 2019, 10, 10122-10128.	7.4	42
38	Ag-Doped Halide Perovskite Nanocrystals for Tunable Band Structure and Efficient Charge Transport. ACS Energy Letters, 2019, 4, 534-541.	17.4	96
39	Emerging Technologies of Flexible Pressure Sensors: Materials, Modeling, Devices, and Manufacturing. Advanced Functional Materials, 2019, 29, 1808509.	14.9	316
40	Hybrid Anodic and Metalâ€Assisted Chemical Etching Method Enabling Fabrication of Silicon Carbide Nanowires. Small, 2019, 15, e1803898.	10.0	31
41	A Facile, Low-Cost Plasma Etching Method for Achieving Size Controlled Non-Close-Packed Monolayer Arrays of Polystyrene Nano-Spheres. Nanomaterials, 2019, 9, 605.	4.1	22
42	Improving Operational Stability of pâ€Type Fieldâ€Effect Transistors by Charge Selective Electrodes: a General Strategy. Advanced Electronic Materials, 2019, 5, 1900055.	5.1	14
43	UV Laserâ€Induced Polyimideâ€toâ€Graphene Conversion: Modeling, Fabrication, and Application. Small Methods, 2019, 3, 1900208.	8.6	76
44	Investigation of Na3V2(PO4)2O2F as a sodium ion battery cathode material: Influences of morphology and voltage window. Nano Energy, 2019, 60, 510-519.	16.0	69
45	Technology Development for Simultaneous Wearable Monitoring of Cerebral Hemodynamics and Blood Pressure. IEEE Journal of Biomedical and Health Informatics, 2019, 23, 1952-1963.	6.3	8
46	Multi-Wavelength Photoplethysmography Enabling Continuous Blood Pressure Measurement With Compact Wearable Electronics. IEEE Transactions on Biomedical Engineering, 2019, 66, 1514-1525.	4.2	76
47	Nanostructured Siliconâ€Based Heterojunction Solar Cells with Double Holeâ€Transporting Layers. Advanced Electronic Materials, 2019, 5, 1800070.	5.1	12
48	An Investigation of Time Difference Between Epidermal Pressure Pulse and PPG Signal. IFMBE Proceedings, 2019, , 185-186.	0.3	0
49	Long-term blood pressure prediction with deep recurrent neural networks. , 2018, , .		108
50	Fusedâ€Ring Electron Acceptor ITICâ€Th: A Novel Stabilizer for Halide Perovskite Precursor Solution. Advanced Energy Materials, 2018, 8, 1703399.	19.5	112
51	Textileâ€Enabled Highly Reproducible Flexible Pressure Sensors for Cardiovascular Monitoring. Advanced Materials Technologies, 2018, 3, 1700222.	5.8	72
52	Probing Photo-Induced Vibrational Kinetics in Perovskite Thin Films. , 2018, , .		0
53	Red Phosphorus: An Elementary Semiconductor for Room-Temperature NO ₂ Gas Sensing. ACS Sensors, 2018, 3, 2629-2636.	7.8	19
54	Comparisons of Oscillometric Blood Pressure Measurements at Different Sites of the Upper Limb. , 2018, 2018, 1168-1171.		3

#	Article	IF	CITATIONS
55	Polarization Sensitive Plasmonic Photodetector Based on HgTe Quantum Dots. , 2018, , .		0
56	Alignmentâ€Free Liquidâ€Capsule Pressure Sensor for Cardiovascular Monitoring. Advanced Functional Materials, 2018, 28, 1805045.	14.9	52
57	Hidden Structure Ordering Along Backbone of Fusedâ€Ring Electron Acceptors Enhanced by Ternary Bulk Heterojunction. Advanced Materials, 2018, 30, e1802888.	21.0	212
58	Highly Sensitive Terahertz Thin-Film Total Internal Reflection Spectroscopy Reveals in Situ Photoinduced Structural Changes in Methylammonium Lead Halide Perovskites. Journal of Physical Chemistry C, 2018, 122, 17552-17558.	3.1	21
59	Wood Derived Composites for High Sensitivity and Wide Linearâ€Range Pressure Sensing. Small, 2018, 14, e1801520.	10.0	79
60	A thermal interface material based on foam-templated three-dimensional hierarchical porous boron nitride. Journal of Materials Chemistry A, 2018, 6, 17540-17547.	10.3	94
61	Compositionâ€Tuned Wide Bandgap Perovskites: From Grain Engineering to Stability and Performance Improvement. Advanced Functional Materials, 2018, 28, 1803130.	14.9	121
62	Spectroscopic Study of Charge Transport at Organic Solid–Water Interface. Chemistry of Materials, 2018, 30, 5422-5428.	6.7	7
63	Interstitial Occupancy by Extrinsic Alkali Cations in Perovskites and Its Impact on Ion Migration. Advanced Materials, 2018, 30, e1707350.	21.0	233
64	Sequentially-processed Na3V2(PO4)3 for cathode material of aprotic sodium ion battery. Nano Energy, 2018, 50, 323-330.	16.0	43
65	High-performance chemical vapor deposited graphene-on-silicon nitride waveguide photodetectors. Optics Letters, 2018, 43, 1399.	3.3	33
66	Quasi-type-II amorphous red phosphorus@TiO2 hybrid films for photoanodic applications. Electrochimica Acta, 2018, 282, 185-193.	5.2	3
67	Recent Advances in Biointegrated Optoelectronic Devices. Advanced Materials, 2018, 30, e1800156.	21.0	76
68	High efficiency ternary organic solar cell with morphology-compatible polymers. Journal of Materials Chemistry A, 2017, 5, 11739-11745.	10.3	74
69	Efficient Red Perovskite Lightâ€Emitting Diodes Based on Solutionâ€Processed Multiple Quantum Wells. Advanced Materials, 2017, 29, 1606600.	21.0	155
70	Low-temperature solution-processed NiO _x films for air-stable perovskite solar cells. Journal of Materials Chemistry A, 2017, 5, 11071-11077.	10.3	113
71	Mercury Telluride Quantum Dot Based Phototransistor Enabling High-Sensitivity Room-Temperature Photodetection at 2000 nm. ACS Nano, 2017, 11, 5614-5622.	14.6	110
72	Flexible Organic/Inorganic Hybrid Nearâ€Infrared Photoplethysmogram Sensor for Cardiovascular Monitoring. Advanced Materials, 2017, 29, 1700975.	21.0	193

#	Article	IF	CITATIONS
73	Flexible Piezoelectric-Induced Pressure Sensors for Static Measurements Based on Nanowires/Graphene Heterostructures. ACS Nano, 2017, 11, 4507-4513.	14.6	435
74	Liquid–Solid Dual-Gate Organic Transistors with Tunable Threshold Voltage for Cell Sensing. ACS Applied Materials & Interfaces, 2017, 9, 38687-38694.	8.0	46
75	Benzylamineâ€Treated Wideâ€Bandgap Perovskite with High Thermalâ€Photostability and Photovoltaic Performance. Advanced Energy Materials, 2017, 7, 1701048.	19.5	188
76	Room Temperature Synthesis of HgTe Quantum Dots in an Aprotic Solvent Realizing High Photoluminescence Quantum Yields in the Infrared. Chemistry of Materials, 2017, 29, 7859-7867.	6.7	27
77	Pulse Transit Time Based Continuous Cuffless Blood Pressure Estimation: A New Extension and A Comprehensive Evaluation. Scientific Reports, 2017, 7, 11554.	3.3	149
78	Hollow‣tructured Graphene–Siliconeâ€Compositeâ€Based Piezoresistive Sensors: Decoupled Property Tuning and Bending Reliability. Advanced Materials, 2017, 29, 1702675.	21.0	213
79	Integrated near-infrared photodetector based on colloidal HgTe quantum dot loaded plasmonic waveguide. , 2017, , .		4
80	Coherence analysis of invasive blood pressure and its noninvasive indicators for improvement of cuffless measurement accuracy. , 2017, 2017, 2255-2258.		3
81	Multi-wavelength photoplethysmography method for skin arterial pulse extraction. Biomedical Optics Express, 2016, 7, 4313.	2.9	77
82	Flexible Piezoresistive Sensor Patch Enabling Ultralow Power Cuffless Blood Pressure Measurement. Advanced Functional Materials, 2016, 26, 1178-1187.	14.9	367
83	Organic Cationâ€Dependent Degradation Mechanism of Organotin Halide Perovskites. Advanced Functional Materials, 2016, 26, 3417-3423.	14.9	229
84	Wearable Sensors: Flexible Piezoresistive Sensor Patch Enabling Ultralow Power Cuffless Blood Pressure Measurement (Adv. Funct. Mater. 8/2016). Advanced Functional Materials, 2016, 26, 1303-1303.	14.9	9
85	Electron Mobility Exceeding 10 cm ² V ^{â^'1} s ^{â^'1} and Bandâ€Like Charge Transport in Solutionâ€Processed nâ€Channel Organic Thinâ€Film Transistors. Advanced Materials, 2016, 28, 5276-5283.	21.0	173
86	An organic water-gated ambipolar transistor with a bulk heterojunction active layer for stable and tunable photodetection. Applied Physics Letters, 2016, 109, .	3.3	7
87	Nitrogen-doped hierarchically porous carbon foam: A free-standing electrode and mechanical support for high-performance supercapacitors. Nano Energy, 2016, 25, 193-202.	16.0	287
88	Photoexcitation dynamics in solution-processed formamidinium lead iodide perovskite thin films for solar cell applications. Light: Science and Applications, 2016, 5, e16056-e16056.	16.6	194
89	Phenylalkylamine Passivation of Organolead Halide Perovskites Enabling Highâ€Efficiency and Airâ€6table Photovoltaic Cells. Advanced Materials, 2016, 28, 9986-9992.	21.0	532
90	Unusual thermal transport behavior in self-assembled fullerene nanorods. RSC Advances, 2016, 6, 67509-67513.	3.6	2

#	Article	IF	CITATIONS
91	Understanding Morphology Compatibility for High-Performance Ternary Organic Solar Cells. Chemistry of Materials, 2016, 28, 6186-6195.	6.7	150

92 Perovskites: Photoluminescence Enhancement in Formamidinium Lead Iodide Thin Films (Adv. Funct.) Tj ETQq0 0 0 1 gBT /Overlock 10 Tf

93	Distribution of bromine in mixed iodide–bromide organolead perovskites and its impact on photovoltaic performance. Journal of Materials Chemistry A, 2016, 4, 16191-16197.	10.3	29
94	Continuous Blood Pressure Measurement From Invasive to Unobtrusive: Celebration of 200th Birth Anniversary of Carl Ludwig. IEEE Journal of Biomedical and Health Informatics, 2016, 20, 1455-1465.	6.3	124
95	A preliminary study on multi-wavelength PPG based pulse transit time detection for cuffless blood pressure measurement. , 2016, 2016, 615-618.		25
96	Dual-modality arterial pulse monitoring system for continuous blood pressure measurement. , 2016, 2016, 5773-5776.		4
97	Thin Film Electrochemical Capacitors Based on Organolead Triiodide Perovskite. Advanced Electronic Materials, 2016, 2, 1600114.	5.1	37
98	Photoluminescence Enhancement in Formamidinium Lead Iodide Thin Films. Advanced Functional Materials, 2016, 26, 4653-4659.	14.9	61
99	Porous PbI ₂ films for the fabrication of efficient, stable perovskite solar cells via sequential deposition. Journal of Materials Chemistry A, 2016, 4, 10223-10230.	10.3	56
100	Native Defectâ€Induced Hysteresis Behavior in Organolead Iodide Perovskite Solar Cells. Advanced Functional Materials, 2016, 26, 1411-1419.	14.9	218
101	Carrier-Activated Polarization in Organometal Halide Perovskites. Journal of Physical Chemistry C, 2016, 120, 2536-2541.	3.1	27
102	Amorphous nanostructured FeOOH and Co–Ni double hydroxides for high-performance aqueous asymmetric supercapacitors. Nano Energy, 2016, 21, 145-153.	16.0	254
103	Flexure-based Roll-to-roll Platform: A Practical Solution for Realizing Large-area Microcontact Printing. Scientific Reports, 2015, 5, 10402.	3.3	36
104	A flexible tonoarteriography-based body sensor network for cuffless measurement of arterial blood pressure. , 2015, , .		13
105	HPbl ₃ : A New Precursor Compound for Highly Efficient Solutionâ€Processed Perovskite Solar Cells. Advanced Functional Materials, 2015, 25, 1120-1126.	14.9	293
106	Facile and scalable fabrication of three-dimensional Cu(OH) ₂ nanoporous nanorods for solid-state supercapacitors. Journal of Materials Chemistry A, 2015, 3, 17385-17391.	10.3	100
107	Template-grown graphene/porous Fe2O3 nanocomposite: A high-performance anode material for pseudocapacitors. Nano Energy, 2015, 15, 719-728.	16.0	116
108	General observation of the memory effect in metal-insulator-ITO structures due to indium diffusion. Semiconductor Science and Technology, 2015, 30, 074002.	2.0	11

#	Article	IF	CITATIONS
109	Low-temperature Ni particle-templated chemical vapor deposition growth of curved graphene for supercapacitor applications. Nano Energy, 2015, 13, 458-466.	16.0	37
110	Solution-Processed Ambipolar Organic Thin-Film Transistors by Blending p- and n-Type Semiconductors: Solid Solution versus Microphase Separation. ACS Applied Materials & Interfaces, 2015, 7, 28019-28026.	8.0	51
111	In Situ Probing of the Charge Transport Process at the Polymer/Fullerene Heterojunction Interface. Journal of Physical Chemistry C, 2015, 119, 25598-25605.	3.1	5
112	Ternary morphology facilitated thick-film organic solar cell. RSC Advances, 2015, 5, 88500-88507.	3.6	27
113	High performance inverted structure perovskite solar cells based on a PCBM:polystyrene blend electron transport layer. Journal of Materials Chemistry A, 2015, 3, 9098-9102.	10.3	192
114	Composition-Dependent Light-Induced Dipole Moment Change in Organometal Halide Perovskites. Journal of Physical Chemistry C, 2015, 119, 1253-1259.	3.1	53
115	Heterojunction with Organic Thin Layers on Silicon for Record Efficiency Hybrid Solar Cells. Advanced Energy Materials, 2014, 4, 1300923.	19.5	100
116	Influence of Donor–Acceptor Arrangement on Charge Transport in Conjugated Copolymers. Journal of Physical Chemistry C, 2014, 118, 5600-5605.	3.1	10
117	Unobtrusive Sensing and Wearable Devices for Health Informatics. IEEE Transactions on Biomedical Engineering, 2014, 61, 1538-1554.	4.2	607
118	Fast, Airâ€&table Infrared Photodetectors based on Sprayâ€Deposited Aqueous HgTe Quantum Dots. Advanced Functional Materials, 2014, 24, 53-59.	14.9	82
119	Ternary Bulk Heterojunction Photovoltaic Cells Composed of Small Molecule Donor Additive as Cascade Material. Journal of Physical Chemistry C, 2014, 118, 20094-20099.	3.1	28
120	Photocurrent Enhancement of HgTe Quantum Dot Photodiodes by Plasmonic Gold Nanorod Structures. ACS Nano, 2014, 8, 8208-8216.	14.6	116
121	High-performance planar heterojunction perovskite solar cells: Preserving long charge carrier diffusion lengths and interfacial engineering. Nano Research, 2014, 7, 1749-1758.	10.4	205
122	The Role of Chlorine in the Formation Process of "CH ₃ NH ₃ PbI _{3â€x} Cl _x ―Perovskite. Advanced Functional Materials, 2014, 24, 7102-7108.	14.9	294
123	Mobile Health: Design of Flexible and Stretchable Electrophysiological Sensors for Wearable Healthcare Systems. , 2014, , .		17
124	Low-voltage graphene field-effect transistors based on octadecylphosphonic acid modified solution-processed high- <i>k</i> dielectrics. Nanotechnology, 2014, 25, 265201.	2.6	4
125	Energy Level Modification in Lead Sulfide Quantum Dot Thin Films through Ligand Exchange. ACS Nano, 2014, 8, 5863-5872.	14.6	843
126	Molecular Packing and Electronic Processes in Amorphous-like Polymer Bulk Heterojunction Solar Cells with Fullerene Intercalation. Scientific Reports, 2014, 4, 5211.	3.3	32

#	Article	IF	CITATIONS
127	Spectral Signature of Intrachain and Interchain Polarons in Donor-Acceptor Copolymers. Acta Chimica Sinica, 2014, 72, 201.	1.4	6
128	Substituent Effects on Physical and Photovoltaic Properties of 5,6-Difluorobenzo[<i>c</i>][1,2,5]thiadiazole-Based D–A Polymers: Toward a Donor Design for High Performance Polymer Solar Cells. Macromolecules, 2013, 46, 9587-9592.	4.8	50
129	Spectroscopic Study of Electron and Hole Polarons in a High-Mobility Donor–Acceptor Conjugated Copolymer. Journal of Physical Chemistry C, 2013, 117, 6835-6841.	3.1	29
130	Quantum dot field effect transistors. Materials Today, 2013, 16, 312-325.	14.2	188
131	A high-sensitivity near-infrared phototransistor based on an organic bulk heterojunction. Nanoscale, 2013, 5, 11850.	5.6	134
132	Low-voltage flexible pentacene thin film transistors with a solution-processed dielectric and modified copper sourceâ \in drain electrodes. Journal of Materials Chemistry C, 2013, 1, 2585.	5.5	12
133	A round robin study of polymer solar cells and small modules across China. Solar Energy Materials and Solar Cells, 2013, 117, 382-389.	6.2	10
134	In situ modification of low-cost Cu electrodes for high-performance low-voltage pentacene thin film transistors (TFTs). Organic Electronics, 2013, 14, 775-781.	2.6	17
135	Limit of Voc in polymeric bulk heterojunction solar cells predicted by a double-junction model. Solar Energy Materials and Solar Cells, 2013, 108, 17-21.	6.2	13
136	A low-temperature, solution-processed high- <i>k</i> dielectric for low-voltage, high-performance organic field-effect transistors (OFETs). Journal Physics D: Applied Physics, 2013, 46, 095105.	2.8	14
137	Bias-Stress Effect in 1,2-Ethanedithiol-Treated PbS Quantum Dot Field-Effect Transistors. ACS Nano, 2012, 6, 3121-3127.	14.6	102
138	Derivitization of pristine graphene for bulk heterojunction polymeric photovoltaic devices. Journal of Materials Chemistry, 2012, 22, 16723.	6.7	16
139	Graphene/Metal Contacts: Bistable States and Novel Memory Devices. Advanced Materials, 2012, 24, 2614-2619.	21.0	32
140	Single crystal n-channel field effect transistors from solution-processed silylethynylated tetraazapentacene. Journal of Materials Chemistry, 2011, 21, 15201.	6.7	48
141	Low-Voltage Organic Field-Effect Transistors (OFETs) with Solution-Processed Metal-Oxide as Gate Dielectric. ACS Applied Materials & amp; Interfaces, 2011, 3, 4662-4667.	8.0	61
142	Heterojunction Photovoltaics Using GaAs Nanowires and Conjugated Polymers. Nano Letters, 2011, 11, 408-413.	9.1	98
143	Inorganic–Organic Hybrid Solar Cell: Bridging Quantum Dots to Conjugated Polymer Nanowires. Nano Letters, 2011, 11, 3998-4002.	9.1	440
144	Device lifetime improvement of polymer-based bulk heterojunction solar cells by incorporating copper oxide layer at Al cathode. Applied Physics Letters, 2011, 98, .	3.3	41

#	Article	IF	CITATIONS
145	Degradation mechanism of organic solar cells with aluminum cathode. Solar Energy Materials and Solar Cells, 2011, 95, 3303-3310.	6.2	65
146	Super-linear rectifying property of rubrene single crystal devices. Organic Electronics, 2011, 12, 1731-1735.	2.6	4
147	Improved Current Extraction from ZnO/PbS Quantum Dot Heterojunction Photovoltaics Using a MoO ₃ Interfacial Layer. Nano Letters, 2011, 11, 2955-2961.	9.1	265
148	Anisotropy of Charge Transport in a Uniaxially Aligned and Chainâ€Extended, Highâ€Mobility, Conjugated Polymer Semiconductor. Advanced Functional Materials, 2011, 21, 932-940.	14.9	166
149	Colloidal PbS Quantum Dot Solar Cells with High Fill Factor. ACS Nano, 2010, 4, 3743-3752.	14.6	416
150	Charge Transport Physics of Conjugated Polymer Fieldâ€Effect Transistors. Advanced Materials, 2010, 22, 3893-3898.	21.0	178
151	Interfacial Recombination for Fast Operation of a Planar Organic/QD Infrared Photodetector. Advanced Materials, 2010, 22, 5250-5254.	21.0	66
152	Control of the Carrier Type in InAs Nanocrystal Films by Predeposition Incorporation of Cd. ACS Nano, 2010, 4, 7373-7378.	14.6	46
153	Local Charge Trapping in Conjugated Polymers Resolved by Scanning Kelvin Probe Microscopy. Physical Review Letters, 2009, 103, 256803.	7.8	61
154	Temperature- and density-dependent channel potentials in high-mobility organic field-effect transistors. Physical Review B, 2009, 80, .	3.2	18
155	Polaron Localization at Interfaces in Highâ€Mobility Microcrystalline Conjugated Polymers. Advanced Materials, 2009, 21, 3759-3763.	21.0	105
156	Downscaling of Organic Fieldâ€Effect Transistors with a Polyelectrolyte Gate Insulator. Advanced Materials, 2008, 20, 4708-4713.	21.0	138
157	Self-aligned inkjet printing of highly conducting gold electrodes with submicron resolution. Journal of Applied Physics, 2007, 101, 064513.	2.5	73
158	Downscaling of self-aligned, all-printed polymer thin-film transistors. Nature Nanotechnology, 2007, 2, 784-789.	31.5	515
159	Self-aligned printing of high-performance polymer thin-film transistors. , 2006, , .		0
160	Molecular-weight dependence of interchain polaron delocalization and exciton bandwidth in high-mobility conjugated polymers. Physical Review B, 2006, 74, .	3.2	262
161	Characterization of MOS Structures Based on Poly (3,3 <tex>\$^primeprimeprime\$</tex> -Dialkyl-Quaterthiophene). IEEE Transactions on Electron Devices, 2005, 52, 2150-2156.	3.0	27
162	Controlled orientation of liquid-crystalline polythiophene semiconductors for high-performance organic thin-film transistors. Applied Physics Letters, 2005, 86, 142102.	3.3	130

#	Article	IF	CITATIONS
163	Microscopic Studies on Liquid Crystal Poly(3,3â€~Ââ€~â€~-dialkylquaterthiophene) Semiconductor. Macromolecules, 2004, 37, 8307-8312.	4.8	86